Pump-Probe Spectroscopy of Exciton Dynamics in (6,5) Carbon Nanotubes

Zipeng Zhu,[†] Jared Crochet,[†] Michael S. Arnold,[‡] Mark C. Hersam,[‡] Hendrik Ulbricht,[§] Daniel Resasco,[||] and Tobias Hertel*[,†,⊥]

Vanderbilt Institute of Nanoscale Science and Engineering, Department of Physics and Astronomy, Vanderbilt University, Nashville, Tennessee, Department of Materials Science and Engineering, Northwestern University, Evanston, Illinois, Institute for Experimental Physics, University of Vienna, Vienna, Austria, and School of Chemical Engineering and Materials Science, University of Oklahoma, Norman, Oklahoma

Received: October 23, 2006; In Final Form: December 19, 2006

We investigate exciton dynamics in isopycnically enriched (6,5) nanotube-DNA suspensions using femtosecond time-resolved pump−probe spectroscopy. The ground state recovery is characterized by a $t^{-0.45 \pm 0.03}$ power law behavior, indicative of a one-dimensional diffusion-limited reaction that is tentatively attributed to subdiffusive trapping of dark excitons. Spectral transients of bright ${}_0A_0^-$ singlet excitons within the E_{11} and E_{22} manifolds exhibit a photobleach (PB) and a photoabsorption (PA) signal of similar strength. The PA is blue-shifted with respect to the PB-signal by 7.5 meV and is attributed to a transition from the dark singlet exciton ${}_0A_0^+$ to a ${}_0A_0^- + {}_0A_0^+$ state within the two exciton E_{11} manifold.

Introduction

The energetics and dynamics of excited states in semiconducting single-wall carbon nanotubes (SWNTs) attract growing attention because of interest in both fundamental and applied aspects of their optical properties.[1] Fundamental interest is stimulated in part by the unique characteristics brought about by the one-dimensional (1D) nature of the electronic states while practical interest is because of the demonstrated use of SWNTs in opto- and nanoelectronic prototype devices.[2,3]

Pump−probe spectroscopy elucidates intriguing characteristics of excited-state dynamics in CNTs that may be associated in part with the peculiarities of electrostatic interactions and transport properties in systems with reduced dimensionality.[4−16] However, difficulties with the overlap of photobleaching (PB) and photoabsorption (PA) signal components in congested spectral regions of polydisperse nanotube suspensions and films remain, making a determination of the E_{11} dephasing and energy relaxation times and other components from pump−probe data difficult. Identification of the PA signal with specific tube types has likewise been complicated by the occurrence of such signals more or less throughout the entire range of transient spectra. Previously reported transients from samples made by the HIPCO technique for example did not allow to identify PA features with specific optical transitions. It could thus not be determined whether the shape of transient spectra was the consequence of a frequency shift of excited-state absorption, a broadening of excited-state spectra, or perhaps a combination of the two.[9] The investigation of spectral transients in chirality enriched samples presented here overcomes such difficulties and facilitates a better understanding of excited-state dynamics and energetics in carbon nanotubes.[17]

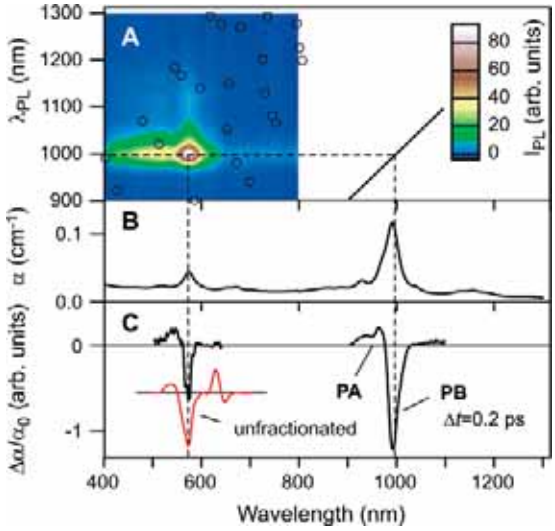

Figure 1. (A) Photoluminescence excitation, (B) ground state absorption, and (C) transient absorption spectra of a (6,5) enriched nanotube suspension. Black circles in the top panel indicate the expected positions of spectral features from other tube species. Both PLE and absorption spectra are dominated by dipole allowed ${}_0A_0^-$ (E_{11}) and ${}_0A_0^-$ (E_{22}) transitions near 993 and 572 nm, respectively. The signal around 625 nm in the unfractionated Comocat sample arises from contributions of the (7,5) tube.

Methods

Nanotube suspensions are prepared using isopycnic fractionation of DNA suspended CoMoCAT raw material as described in ref 18. Chirality enrichment of the resulting purple-tinted samples is evident from photoluminescence excitation (PLE) and linear absorption spectra in Figure 1A,B which are dominated by the bright ${}_0A_0^-$ singlet excitons (line group notation, see ref 19) within the (6,5) E_{11} and E_{22} manifolds at 993 and 572 nm, respectively. Pump−probe experiments are performed using the signal and idler as well as the white-light continuum output of a Ti/Sapphire laser driven optical para-

* Corresponding author. E-mail: tobias.hertel@vanderbilt.edu.
[†] Department of Physics and Astronomy, Vanderbilt University.
[‡] Northwestern University.
[§] University of Vienna.
[||] University of Oklahoma.
[⊥] Vanderbilt Institute of Nanoscale Science and Engineering.

10.1021/jp0669411 CCC: $37.00
Published on Web 02/21/2007

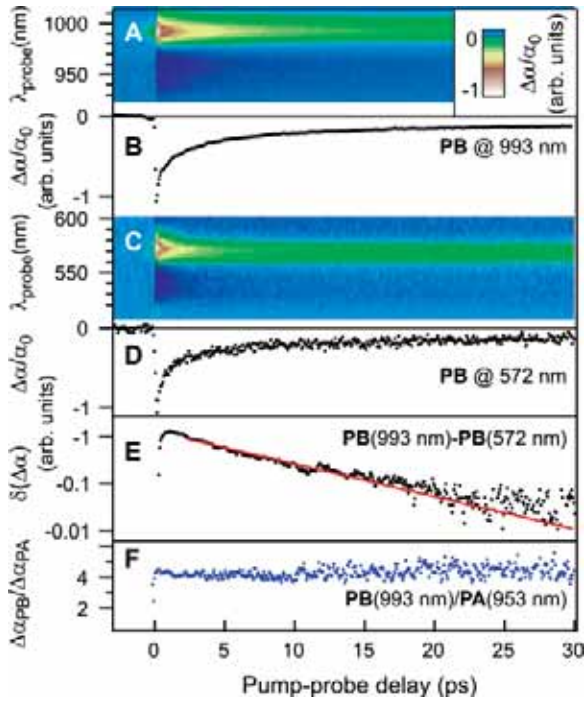

Figure 2. (A) and (C) spectra transients in the ${}_0A_0^-$ (E_{11}) and ${}_0A_0^-$ (E_{22}) wavelength range after resonant excitation of the E_{11} transition. The corresponding on resonant PB dynamics are seen in (B) and (D). The strength of the PB at 993 nm in (C) and (D) is only slightly smaller than that in (A) and (B). (E) The difference of normalized PB transients in (B) and (D) reflects the ${}_0A_0^-$ (E_{11}) excited-state population. (F) The constant ratio of this transient indicates that recovery of all features is governed by the same mechanism.

metric amplifier. Optical transients $\Delta\alpha/\alpha_0$ are measured with a sensitivity of up to 2×10^{-6} using phase sensitive detection. More details about the experimental setup and sample preparation can be found elsewhere.[18,20]

At the wavelengths used in this study, photoabsorption cross sections of the $\pi-\pi^*$ continuum in sp^2 hybridized polyaromatic hydrocarbon compounds are on the order of 1×10^{-18} cm^2 atom^{-1}.[21] This suggests that at least 1.5 photons are absorbed per 100 nm of tube length at typical pump fluences of 1.5×10^{14} cm^{-2}. We speculate, however, that the actual absorption cross section at exciton resonances is enhanced significantly with respect to the above estimate because of the spectral dominance of excitonic transitions in 1D systems.[22−24] In fact, the large number of atoms in a nanotube makes it experimentally challenging to perform experiments at fluences that on average would lead to less than one excitation per tube.

Figure 1C shows transient spectra at 0.2 ps delay after resonant excitation of the ${}_0A_0^-$ singlet exciton of the E_{22} manifold at 572 nm. The transients are characterized by a dominant PB at the resonance energy of ${}_0A_0^-$ excitons in both E_{11} and E_{22} manifolds as well as by a blue-shifted PA signal. We find no evidence for transitions to a red-shifted singlet biexciton state, which has been predicted to lead to red-shifted PA features.[25] Qualitatively similar behavior is observed for resonant excitation of the ${}_0A_0^-$ (E_{11}) exciton at 993 nm and transient spectra in Figure 2A,C are likewise characterized by PB and blueshifted PA signals at the ${}_0A_0^-$ transition energies of E_{11} and E_{22} manifolds. The peculiar occurrence of optical transients near 2.15 eV after excitation at 1.24 eV in Figure 2C,D, however, requires a closer look at the differential absorbance $\Delta\alpha$, which (neglecting coherent effects) is given by

$$\Delta\alpha_{fi} = \hat{C}_{fi}(\Delta\hat{\rho}_{ii} - \Delta\hat{\rho}_{ff}) \quad (1)$$

The indices i and f refer to initial and final states respectively and $\hat{C}_{fi}$ is a constant that is proportional to the transition dipole moment μ_{fi}. The population of different states can be described using the density matrix, whose elements $\hat{\rho}_{lm}$ refer to the population and coherences of ground state and the dressed two-particle exciton states. Resonant excitation of the ${}_0A_0^-$ exciton in the E_{11} manifold leads to an increase of population in the excited state $\Delta\hat{\rho}_{11} > 0$ and a decrease of the ground state ${}_0A_0^+$ (GS) population (i.e., $\Delta\hat{\rho}_{00} < 0$). As a consequence, the change of the absorbance for the ${}_0A_0^-$ (E_{11}) $\leftarrow$ ${}_0A_0^+$ (GS) transition, $\Delta\alpha_{10} = \hat{C}_{10}(\Delta\hat{\rho}_{00} - \Delta\hat{\rho}_{11})$ is negative, which is referred to as PB. Evidently, the reduction of the ground state population also gives rise to a bleach signal at the ${}_0A_0^-$ (E_{22}) $\leftarrow$ ${}_0A_0^+$ (GS) transition, even if the respective excited-state population $\hat{\rho}_{22}$ is 0. As will be explained in the following paragraph, the PB dynamics at the second subband exciton transition therefore determines the ground state population dynamics (see Figure 2C,D). The linear pump power dependence of all transients (not shown) likewise indicates that singlet biexciton annihilation or Auger recombination do not contribute to the population dynamics of the E_{22} exciton at the pump fluences used here.

Results and Discussion

In the following, we briefly outline how the ${}_0A_0^-$ (E_{11}) state population dynamics can be obtained from the E_{11} and E_{22} transients here designated as $\Delta\alpha_{10}$, and $\Delta\alpha_{20}$, respectively. According to eq 1, these transients can be simplified to $\Delta\alpha_{10} = \hat{C}_{10}\Delta\hat{\rho}_{00}$ and $\Delta\alpha_{20} = \hat{C}_{20}\Delta\hat{\rho}_{00}$ for times t much larger than T_1, the energy relaxation time of the ${}_0A_0^-$ (E_{11}) and ${}_0A_0^-$ (E_{22}) states (i.e., at times when $\hat{\rho}_{11}$ and $\hat{\rho}_{22}$ have practically returned to zero). Experimentally, this situation can be identified by the synchronous decay of both transients, which is found at pump−probe time delays in excess of about 50 ps. Normalization of these transients (e.g., at 50 ps) then extracts $\Delta\hat{\rho}_{11}$ from the difference of the normalized transients $\delta(\Delta\tilde{\alpha}(t)) \equiv \Delta\alpha_{10}(t) - \Delta\alpha_{20}(t) = \tilde{C}[\Delta\hat{\rho}_{22}(t) - \Delta\hat{\rho}_{11}(t)]$ that provides us with a direct measure of the ${}_0A_0^-$ (E_{11}) state population once it is safe to assume that the E_{22} population has decayed completely .[11] The result shown in Figure 2E exhibits a nearly monoexponential decay with a time-constant of (6 ± 1) ps. Time-resolved PL studies have indeed shown that the ${}_0A_0^-$ (E_{11}) excitation decays within a few tens of picoseconds,[10,32] which is consistent with our observations.

The long-term dynamics of PA and PB transients, irrespective of the pump-wavelength, follows power law scaling according to $\Delta\alpha/\alpha_0 \propto t^{-\beta}$. A fit to the tails of PB or PA signals in chirality enriched samples yields an exponent $\beta = 0.45 \pm 0.03$ up to at least 0.8 ns (see Figure 3). This exponent is independent of pump power, even at fluences where the short-term dynamics are believed to be affected by singlet−singlet interactions.[10,13,26] In contrast, significant deviations from $\beta = 0.45$ scaling are found in unfractionated or bundled samples.

A power-law dependence of transients on time strongly suggests that the ground state recovery is diffusion limited.[28] In low-dimensional systems, the recombination rate for particle−particle or particle-antiparticle reactions is known to vary with dimensionality and particle density. In the case of SWNTs where excitons are more or less delocalized over the circumference of the nanotube, it is safe to assume that the system behaves

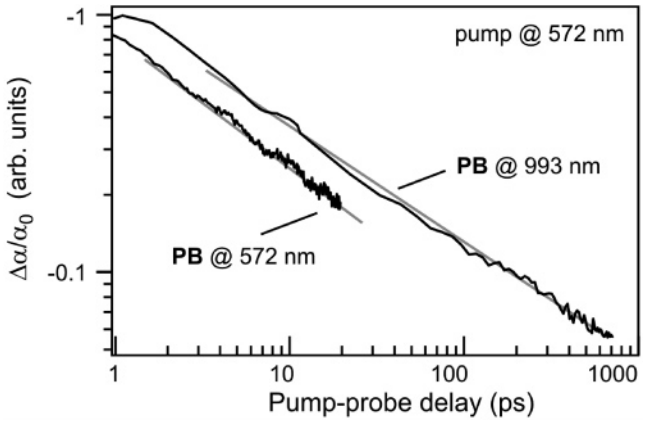

Figure 3. The long term dynamics of PA and PB signals are characterized by a common power law indicative of diffusion-limited ground state recovery.

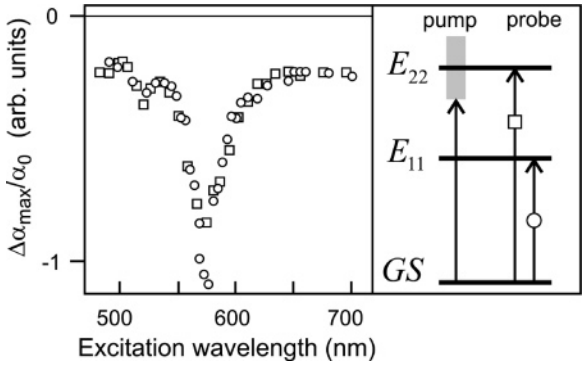

Figure 4. Dependence of ${}_0A_0^-$ (E_{11}) and ${}_0A_0^-$ (E_{22}) cross-correlation maxima on pump wavelength. The feature at 525 nm is attributed to a *G*-mode phonon sideband by analogy to phonon sidebands found in PL excitation spectra.

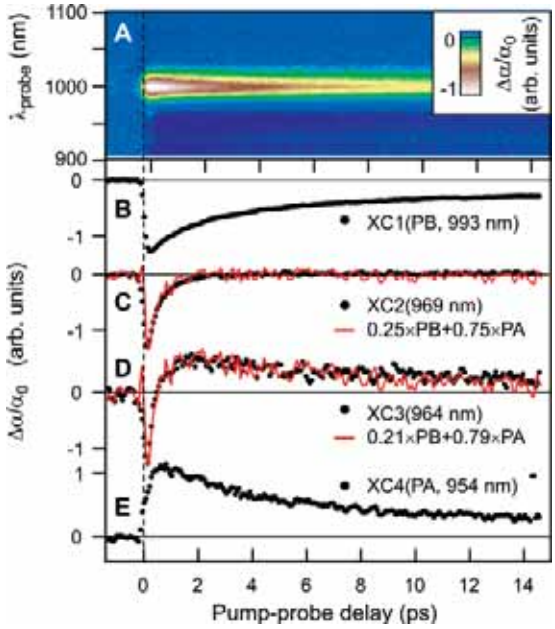

Figure 5. (A-E) Wavelength dependence of ${}_0A_0^-$ (E_{11}) transients after excitation of the ${}_0A_0^-$ (E_{22}) exciton. (B-E) Traces at wavelengths intermediate to those at the PB and PA extrema can be described by an incoherent superposition of PB and PA signals.

one-dimensionally with respect to its diffusive properties.[13] The 1D diffusion-limited reactions of the type $A + A \rightarrow B$, as expected if the ground state recovery were limited by a diffusive annihilation reaction involving dark singlet excitons,[23,24,27] for example, are characterized by $\beta = 1/4$,[28] contrary to our observations. Particle−antiparticle annihilation reactions $A + \bar{A} \rightarrow C$ on the other hand are known to have a 1D scaling behavior with $\beta = 1/2$, close to the exponent found here.[28] Such behavior would be expected for radiative recombination of free electrons and holes, which for example would clearly be at variance with the excitonic nature of these optical transitions. Triplet−triplet annihilation in which excitons with spin up and down would take on the role of particle and antiparticle, respectively, could possibly also explain $\beta = 1/2$ scaling. However, this is difficult to reconcile with the early (sub 10 ps) onset of the power law decay because intersystem-crossing rates in such systems are assumed to be orders of magnitude smaller.

Survival probabilities for subdiffusive trapping $A + Tr \rightarrow Tr^*$ in disordered 1D systems on the other hand scale with $t^{-\gamma}$ with $0 < \gamma < 1$, where t^{-1} would be observed for Fickian diffusion.[29] The observed scaling is thus compatible with subdiffusive exciton trapping in which the mean square displacement of carriers due to the particles random walk would be described by $\langle r^2(t) \rangle \propto t^{-0.45}$. Once trapped, the excitation decays rapidly (i.e., within less than about 10 ps) to allow the ground state population to follow the observed nonexponential scaling behavior of the trapping rate.

To analyze the origin of optical transients in further detail, we also studied the strength of the PB signal at 993 and 572 nm as a function of excitation wavelength. The results are shown in Figure 4 where the maximum of the differential absorbance at the ${}_0A_0^-$ (E_{11}) and ${}_0A_0^-$ (E_{22}) exciton resonances is plotted versus the excitation wavelength. Apart from the pronounced resonant enhancement of (6,5) transients at the ${}_0A_0^-$ (E_{22}) energy, we also find a weak sideband around 525 nm, which is attributed to *G*-mode phonon replica.[30] Similarly interesting is the constant background at wavelengths in which no features are observed in optical transients (e.g., between 650 and 700 nm). This suggests that the response for excitation at these wavelengths might be associated with nonresonant excitation of a state that rapidly dephases by decay to lower lying levels. This nonresonantly excited-state could for example be the π-plasmon resonance around 5.2 eV that is also believed to dominate the nonresonant background of the ground state absorption spectrum (see Figure 1B).[31]

We now turn to a discussion of the nature of the PA feature. In Figure 5 we illustrate how the complex wavelength dependence of transients, here for excitation at 572 nm, can be decomposed into a simple incoherent superposition of PB and PA signal components extracted at 993 and 954 nm, respectively, (see Figure 5B−E). In contrast to excitation at 993 nm, PB and PA transients here exhibit slightly different rise times. Evidently the superposition of such transients can lead to cross-correlations with nearly arbitrary behavior from very fast decay at 969 nm (Figure 5C) to the complex behavior at slightly shorter wavelengths (Figure 5D). Quantitative evaluation of transients in polydisperse samples thus seems particularly daunting. In essence, this shows that the PA signal is probably caused by a distinct optical transition whose recovery is nevertheless nearly identical to that of the transition giving rise to the PB signal components. In the frequency domain, this is supported by the fit to the optical transient in Figure 6 using a linear superposition of Voigt lines with similar intensity for the PB and a blue-shifted PA signal at 993 and 987 ± 2 nm, respectively.

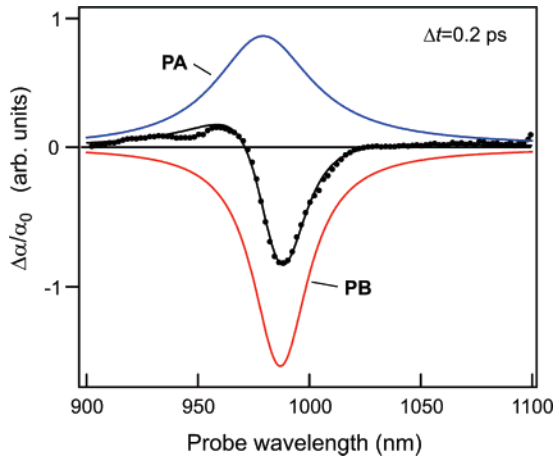

Figure 6. Transient spectra can be decomposed into a superposition of a PB and a PA Voigt profile.

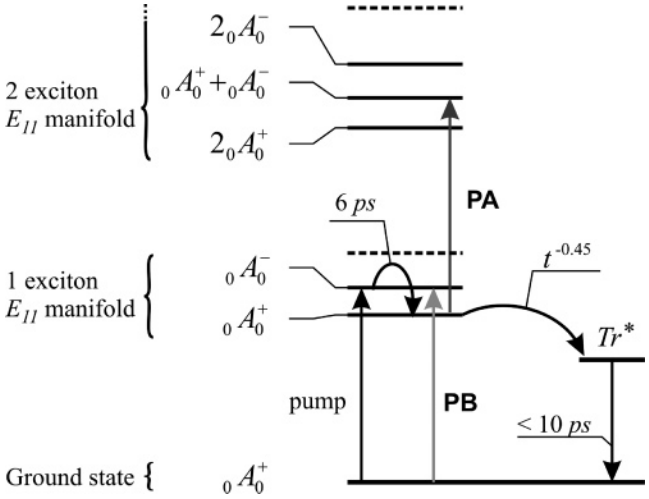

Figure 7. Schematic energy level scheme for exciton dynamics in SWNTs. The transition from the GS to the dipole allowed ${}_0A_0^-$ (E_{11}) exciton is PB after excitation with a 993 nm pump pulse. The bright ${}_0A_0^-$ (E_{11}) exciton then rapidly decays within 6 ps to the dark state ${}_0A_0^+$ (E_{11}). The PA signal is attributed to a transition (blue-shifted by 7.5 meV with respect to the PB signal) from the dark state ${}_0A_0^+$ to ${}_0A_0^+ + {}_0A_0^-$ within the two exciton manifold. The bottleneck for GS recovery is tentatively assigned to diffusive trapping of ${}_0A_0^+$ dark excitons by *Tr**. Higher lying states within each manifold are indicated by dashed lines.

The nature of the PA signal is clarified by investigation of the ratios of PB and PA differential absorbances that are found to be constant at pump−probe delays exceeding a few ps (Figure 2F). These observations suggest that the long-term decay of PB and PA is governed by the dynamics of one and the same state although both features belong to different transitions. The persistence of PB and PA signals up to hundreds of ps, moreover indicates that excited-state absorption does not occur directly from the ${}_0A_0^-$ (E_{11}) exciton state because this decays on a time scale of a roughly 6 ps.[10,32]

Summary

A tentative level scheme to account for our findings is shown in Figure 7. It is here constrained to transitions within the one and two E_{11} exciton manifolds and resembles schemes set forth by Marty et al. or Sleferyan et al.[2,16] Within this excitation scheme, photobleaching is due to transitions from the GS to the one E_{11} exciton manifold, ${}_0A_0^-$ (E_{11}) ← ${}_0A_0^+$ (GS). Further decay is accompanied by a rapid decay into lower lying states, such as the lowest lying dark singlet state ${}_0A_0^+$ (E_{11}) with a 6 ± 1 ps time constant. The longer term dynamics is most readily accounted for by subdiffusive trapping of dark excitons ${}_0A_0^+$ (E_{11}) whose mean square displacement increases subdiffusively with $\langle r^2(t)\rangle \propto t^{-0.45}$ because of disorder. Excited-state absorption features are consistent with excitation to a state in the two exciton manifold according to ${}_0A_0^-$ (E_{11}) + ${}_0A_0^+$ (E_{11}) ← ${}_0A_0^+(E_{11})$, which appears to be blue-shifted by 60 ± 20 cm^{-1} with respect to the ${}_0A_0^-$ (E_{11}) ← ${}_0A_0^+$ (GS) transition. The nature of this transition and the associated interactions need to be explored in further detail.

Acknowledgment. Z.Z. acknowledges support by the National Science Foundation (DMR0606505). H.U. acknowledges a Postdoctoral fellowship of the Max-Kade foundation and J.C. acknowledges support through a graduate fellowship of the IGERT program (DGE0333392) as well as a grant by the Petroleum Research Fund (PRF 44479-AC10). M.C.H. acknowledges support from the NSF through EEC0118025 and DMR0134706.

References and Notes

(1) Ando, T.; *J. Phys. Soc. Jap*. **1997**, *66*, 1066.
(2) Marty, L.; Adam, E.; Albert, L.; Doyon, R.; Menard, D. Martel, R. *Phys. Rev. Lett.* **2006**, *96*, 136803.
(3) Derycke, V.; Martel, R.; Appenzeller, J.; Avouris, P. *Nano Lett.* **2001**, *1*, 453.
(4) Ichida, M.; Hamanaka, Y.; Kataura, H.; Achiba, Y.; Nakamura, A. *Physica B* **2002**, *323*, 237.
(5) Lauret, J. S.; Voisin, C.; Cassabois, G.; Delalande, C.; Roussignol, P.; Jost, O.; Capes, L. *Phys. Rev. Lett.* **2003**, *90*, 057404.
(6) Ostojic, G. N.; Zaric, S.; Kono, J.; Strano, M. S.; Moore, V. C.; Hauge, R. H.; Smalley, R. E. *Phys. Rev. Lett.* **2004**, *92*, 117402.
(7) Korovyanko, O. J.; Sheng, C. X.; Vardeny, Z. V.; Dalton, A. B.; Baughman, R. H. *Phys. Rev. Lett.* **2004**, *92*, 017403.
(8) Styers-Barnett, D. J.; Ellison, S. P.; Park, C.; Wise, K. E.; Papanikolas, J. M. *J. Phys. Chem. A* **2005**, *109*, 289.
(9) Ostojic, G. N.; Zaric, S.; Kono, J.; Moore, V. C.; Hauge, R. H.; Smalley, R. E. *Phys. Rev. Lett.* **2005**, *94*, 97401.
(10) Ma, Y. Z.; Valkunas, L.; Dexheimer, S. L.; Bachilo, S. M.; Fleming, G. R. *Phys. Rev. Lett.* **2005**, *94*, 157402.
(11) Manzoni, C.; Gambetta, A.; Menna, E.; Meneghetti, M.; Lanzani, G.; Cerullo, G. *Phys. Rev. Lett.* **2005**, *94*, 270401.
(12) Chou, S. G.; DeCamp, M. F.; Jiang, J.; Samsonidze, G. G.; Barros, E. B.; Plentz, F.; Jorio, A.; Zheng, M.; Onoa, G. B; Semke, E. D.; Tokmakoff, A.; Saito, R.; Dresselhaus, G.; Dresselhaus, M. S. *Phys. Rev. B* **2005**, *72*, 195415.
(13) Valkunas, L.; Ma, Y. Z.; Fleming, G. R. *Phys. Rev. B.* **2006**, *73*, 115432.
(14) Huang; L. B.; and Krauss, T. D. *Phys. Rev. Lett.* **2006**, *96*, 057407.
(15) Perfetti, L.; Kampfrath, T.; Schapper, F.; Hagen, A.; Hertel, T.; Aguirre, C. M.; Desjardins, P.; Martel, R.; Frischkorn, C.; Wolf, M. *Phys. Rev. Lett.* **2006**, *96*, 027401.
(16) Seferyan, H. Y.; Nasr, M. B.; Senekerimyan, V.; Zadoyan, R.; Collins, P.; Apkarian, V. A. *Nano Lett.* **2006**, *6*, 1757.
(17) Perebeinos, V.; Tersoff, J.; Avouris, P. *Nano Lett.* **2005**, *5*, 2495.
(18) Arnold, M. S.; Stupp, S. I.; Hersam, M. C. *Nano Lett.* **2005**, *5*, 713.
(19) Barros, E. B.; Capaz, R. B.; Jorio, A.; Samsonidze, G. G.; Souza Filho, A. G.; Ismail −Beigi, S.; Spataru, C. D.; Dresselhaus, G.; Dresselhaus, M. S. *Phys. Rev. B* **2006**, *73*, 241406.
(20) Resasco, D. E.; Alvarez, W. E.; Pompeo, F.; Balzano, L.; Herrera, J. E.; Kitiyanan, B.; Borgna, A. A. *J. Nanopart. Res.* **2002**, *4*, 131.
(21) Malloci, G.; Mulas, G.; Joblin, C. *Astron. Astrophys.* **2004**, *426*, 105.
(22) Ogawa T.; Takagahara, T. *Phys. Rev. B* **1991**, *43*, 14325.
(23) Perebeinos, V.; Tersoff, J.; Avouris, P. *Phys. Rev. Lett.* **2004**, *92*, 257402.
(24) Spataru, C. D.; Ismail-Beigi, S.; Benedict, L. X.; Louie, S. G. *Phys. Rev. Lett.* **2004**, *92*, 77402.

(25) Pedersen, T. G.; Pedersen, K.; Cornean, H. D.; Duclos, P. *Nano Lett.* **2005**, *5*, 291.
(26) Wang, F.; Dukovic, G.; Knoesel, E.; Brus, L. E.; Heinz, T. F. *Phys. Rev. B.* **2004**, *70*, 241403.
(27) Zhao H.; Mazumdar, S. *Phys. Rev. Lett.* **2005**, *93*, 157402.
(28) Toussaint D.; Wiczek, F. *J. Chem. Phys.* **1983**, *78*, 2642.
(29) Yuste S. B.; Acedo, L. *Physica A* **2004**, *336*, 334.
(30) Htoon, H.; O'Connell, M. J.; Cox, P. J.; Doorn, S. K.; Klimov, V. I. *Phys. Rev. Lett.* **2004**, *93*, 93.
(31) Pichler, T.; Knupfer, M.; Golden, M. S.; Fink, J.; Rinzler, A.; Smalley, R. E. *Phys. Rev. Lett.* **1998**, *80*, 4729.
(32) Hagen, A.; Steiner, M.; Raschke, M. B.; Lienau, Ch.; Hertel, T.; Qian, H.; Meixner, A. J.; Hartschuh, A. *Phys. Rev. Lett.* **2005**, *95*, 197401.